The far-infrared laser magnetic resonance spectrum of the SiH radical and determination of ground state parameters[a)]

John M. Brown[b)]
Department of Chemistry, Southampton University, Southampton S09 5NH, England

Robert F. Curl
Department of Chemistry, Rice University, Houston, Texas 77251

Kenneth M. Evenson
National Bureau of Standards, Boulder, Colorado 80303

(Received 23 April 1984; accepted 15 May 1984)

The far-infrared laser magnetic resonance (LMR) spectrum of the SiH radical in the $v = 0$ level of its $X\,^2\Pi$ state has been recorded. The signals are rather weak. The molecules were generated in the reaction between fluorine atoms and SiH_4. Rotational transitions have been detected in both $^2\Pi_{1/2}$ and $^2\Pi_{3/2}$ spin components but no fine structure transitions between the spin components were observed. Proton hyperfine splittings were resolved on some lines. The measurements have been analyzed, subjected to a least-squares fit using an effective Hamiltonian and the appropriate molecular parameters determined. The weakness of the spectrum and the failure of attempts to power saturate favorable lines are both consistent with a small value for the electric dipole moment for SiH.

I. INTRODUCTION

The SiH radical is much more than a poor relative of CH. It is an important molecule in its own right for several reasons. For example, there is widespread interest in the chemistry of silicon and the role that SiH plays in this area needs to be more clearly defined. Again, the cosmic abundances of hydrogen and silicon suggest that silicon hydrides should be quite plentiful in the regions between and around the stars[1] and radio astronomers in particular are eager to establish the presence of such molecules there.

Precise information on the energy levels of the SiH radical in its ground $^2\Pi$ state has proved particularly hard to obtain in the laboratory. For many years, the optical spectrum has been the sole source of such information.[2,3] Of the various techniques available for the study of free radicals, laser magnetic resonance (LMR) has shown itself to be very sensitive, particularly at far-infrared wavelengths.[4,5] For example, the CH radical has now been extensively studied by LMR spectroscopy[6,7,8] and an equally thorough investigation of the CH_2 radical has recently been completed.[9] It was therefore rather surprising that previous attempts to detect SiH by LMR spectroscopy had been unsuccessful.

We have recently detected transitions in the GeH radical by LMR spectroscopy with good signal-to-noise ratios; details of our observations and their analysis are to be published elsewhere.[10] In these experiments, the GeH molecules were generated by the reaction between F atoms and germane (GeH_4). Since this was the analogous reaction to that used to generate CH in the later LMR studies[7,8] we have been encouraged to try once again to detect SiH in the reaction of F atoms with silane (SiH_4). The present attempt has proved successful. We report here the observations of transitions in ^{28}SiH in the $v = 0$ level of the $X\,^2\Pi$ state (^{28}Si is present to the extent of 92.3% in natural abundance). By comparison with the LMR spectra of both CH and GeH, the signals are surprisingly weak and it is understandable that they were not detected in earlier work. The results have been analyzed and fitted to a model Hamiltonian to determine the ground state parameters. In consequence, we have been able to make much more reliable estimates of the lambda doubling and rotational frequencies for ^{28}SiH at zero magnetic field to aid extraterrestrial searches for the molecule.[11]

Following these observations at far-infrared wavelengths, the same method of generation has been used in a study of the vibration-rotation spectrum of SiH by CO laser magnetic resonance.[12] Lines in the (1,0) and (2,1) bands of SiH have also been observed recently, recorded in emission from an electric discharge through silane with a Fourier transform interferometer.[13]

II. EXPERIMENTAL DETAILS AND OBSERVATIONS

The spectra were recorded on a comparatively new LMR spectrometer constructed in the Boulder laboratories of the National Bureau of Standards; a detailed description of this apparatus has been given elsewhere.[9] We believe that it is the extra sensitivity afforded by this spectrometer which has made the present observations possible. The SiH radicals were formed in the spectrometer sample volume by the reaction of fluorine atoms with silane, the fluorine atoms being generated by passing a mixture of He and F_2 through a microwave discharge. The optimum pressures were 225, 25, and 5 m Torr of He, F_2, and SiH_4, respectively, conditions which corresponded approximately to a maximum in the purple chemiluminescence.

The radical was first detected using the 117.7 μm line of CH_2F_2, on the basis of predictions from the optical spectrum.[3] At this stage the molecular parameters were refined and the near coincidences between SiH transition frequen-

[a)] Work supported in part by NASA contract W-15, 047.
[b)] Present address: Physical Chemistry Laboratory, South Parks Road, Oxford OX1 3QZ, England.

 0021-9606/84/192884-07$02.10

TABLE I. Summary of observations in the far-infrared LMR spectrum of the ^{28}SiH radical in its ground state.

Pump	Laser line: Gain medium	Laser line: λ/μm	ν/GHz	SiH transition: Ω	SiH transition: J
10P(14)	DCOOH	479.9	624.6926(6)[a,b]	$^2\Pi_{1/2}$	$1\frac{1}{2} \leftarrow \frac{1}{2}$
10P(24)	CD_3OH	286.7	1045.5780(5)[c]	$^2\Pi_{1/2}$	$2\frac{1}{2} \leftarrow 1\frac{1}{2}$
9P(20)	CH_2F_2	159.0	1885.9593(10)[d]	$^2\Pi_{1/2}$	$4\frac{1}{2} \leftarrow 3\frac{1}{2}$
9P(24)	CH_2F_2	256.0	1170.9410(6)[d]	$^2\Pi_{3/2}$	$2\frac{1}{2} \leftarrow 1\frac{1}{2}$
9R(32)	CH_2F_2	184.3	1626.6026(8)[d]	$^2\Pi_{3/2}$	$3\frac{1}{2} \leftarrow 2\frac{1}{2}$
9P(10)	CH_2DOH	183.6	1632.6669(8)[e]	$^2\Pi_{3/2}$	$3\frac{1}{2} \leftarrow 2\frac{1}{2}$
9R(20)	CH_2F_2	117.7	2546.4950(13)[d]	$^2\Pi_{3/2}$	$5\frac{1}{2} \leftarrow 4\frac{1}{2}$

[a] The figures in parentheses give the estimated uncertainty in the laser frequency, in units of the last quoted decimal place.
[b] S. F. Dyubko, A. V. Svich, and L. D. Fesenko, Sov. Phys. Tech. Phys. **20**, 1536 (1976).
[c] K. M. Evenson, F. R. Peterson, and D. A. Jennings (to be published).
[d] F. R. Peterson, A. Scalabrin, and K. M. Evenson, Int. J. IR mm Waves **1**, 111 (1980).
[e] A. Scalabrin, F. R. Peterson, K. M. Evenson, and D. A. Jennings, Int. J. IR mm Waves **1**, 117 (1980).

cies (at zero field) and suitable laser lines were calculated. Detailed predictions of the magnetic resonance spectra for these laser lines were then used as the basis for all subsequent searches. The results are summarized in Table I and are also shown in the energy level diagram in Fig. 1. The signals were in all cases weak with a signal-to-noise ratio of at best 50:1 for a 0.3 s output time constant. The spectrum recorded with the 256.0 μm laser line involving the $^2\Pi_{3/2}$ $J = 2\frac{1}{2} \leftarrow 1\frac{1}{2}$ transition is shown in Fig. 2. We made a number of attempts to saturate the signals by lowering both the total pressure and the modulation amplitude but no Lamb dips were observed. This is in marked contrast to the studies of the CH[8] and GeH[10] radicals where saturation dips were readily observed.

The magnetic flux densities for individual lines were measured from the direct readout of a rotating coil system which was used to control the magnet of the LMR spectrometer. The system was calibrated periodically with a proton NMR gaussmeter up to 1.8 T. The overall uncertainty is 10^{-5} T below 0.1 T, and the fractional uncertainty is 10^{-4} above 0.1 T. The detailed results of these measurements are given in Table II. The proton hyperfine interaction causes a characteristic doubling of all lines involving levels in the $^2\Pi_{1/2}$ spin component. The corresponding splittings for the $^2\Pi_{3/2}$ transitions were much smaller and were only resolved in a few favorable cases (see Table II).

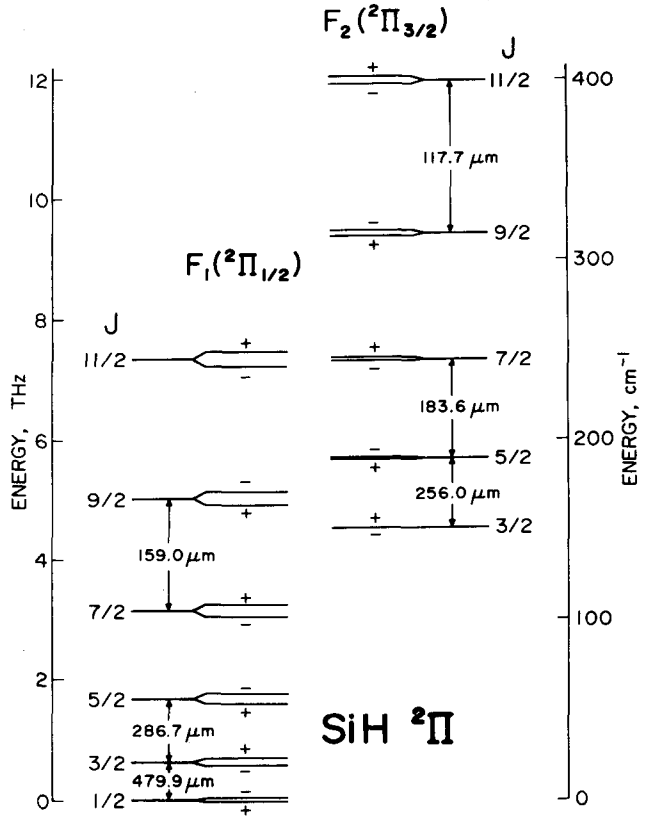

FIG. 1. Diagram showing the lower energy levels of SiH in the $X\,^2\Pi$ state and the transitions involved in the observed far-infrared LMR spectrum. The lambda-type (parity) doubling has been exaggerated by a factor of 20 for clarity.

III. ANALYSIS

The LMR spectra of the SiH radical were assigned with the help of a predictive computer program which has been described earlier.[14] The rotational quantum numbers could be assigned simply by a comparison of the molecular transi-

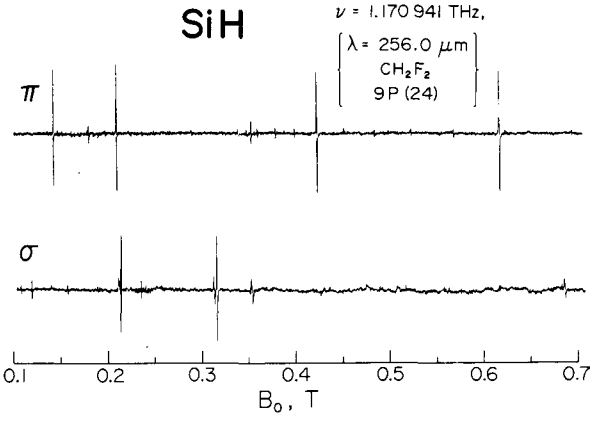

FIG. 2. The 256.0 μm LMR spectrum of the SiH radical, in parallel (π) and perpendicular (σ) polarization. The rotational transition involved is $J = 2\frac{1}{2} \leftarrow 1\frac{1}{2}$ in the $^2\Pi_{3/2}$ component. The spectrum was recorded with a time constant of 0.1 s; it is remarkable for its weakness.

TABLE II. Flux densities and frequencies of transitions observed by LMR for ^{28}SiH in the $X\,^2\Pi$ state.

Parity[a]	M'_J	M_J	M'_I	M_I	Flux density (mT)	$\nu_L - \nu_{calc}$[b] (MHz)	Weight (MHz^{-2})	$\partial\nu/\partial B_0$[b] (MHz/G)
479.9 μm spectrum	$^2\Pi_{1/2}$,	$J = 1\frac{1}{2} \leftarrow \frac{1}{2}$	$\nu_L = 624.6926$ GHz					
Parallel polarization (π)								
$- \leftarrow +$	$-\frac{1}{2}$	$-\frac{1}{2}$	$-\frac{1}{2}$	$-\frac{1}{2}$	341.16	0.27	1.00	−0.067
			$\frac{1}{2}$	$\frac{1}{2}$	352.19	0.26	1.00	−0.067
Perpendicular polarization (σ)								
$- \leftarrow +$	$-1\frac{1}{2}$	$\frac{1}{2}$	$\frac{1}{2}$	$-\frac{1}{2}$	106.26	0.35	1.00	−0.220
	$-1\frac{1}{2}$	$-\frac{1}{2}$	$-\frac{1}{2}$	$-\frac{1}{2}$	108.57	0.24	1.00	−0.210
			$\frac{1}{2}$	$\frac{1}{2}$	113.97	0.54	1.00	−0.211
	$-\frac{1}{2}$	$\frac{1}{2}$	$\frac{1}{2}$	$\frac{1}{2}$	310.60	0.08	1.00	−0.074
			$-\frac{1}{2}$	$-\frac{1}{2}$	315.63	0.26	1.00	−0.073
$+ \leftarrow -$	$-1\frac{1}{2}$	$-\frac{1}{2}$	$\frac{1}{2}$	$\frac{1}{2}$	1415.33	0.10	1.00	−0.213
			$-\frac{1}{2}$	$-\frac{1}{2}$	1417.61	1.95	1.00	−0.213
286.7 μm spectrum	$^2\Pi_{1/2}$,	$J = 2\frac{1}{2} \leftarrow 1\frac{1}{2}$	$\nu_L = 1045.5780$ GHz					
Parallel polarization (π), Perpendicular polarization (σ)	No transitions observed below 2.0 T							
$- \leftarrow +$	$-2\frac{1}{2}$	$-1\frac{1}{2}$	$-\frac{1}{2}$	$-\frac{1}{2}$	375.5	−0.26	1.00	−0.178
			$\frac{1}{2}$	$\frac{1}{2}$	378.1	−0.08	1.00	−0.178
	$-1\frac{1}{2}$	$-\frac{1}{2}$	$-\frac{1}{2}$	$-\frac{1}{2}$	412.74	−0.26	0.50	−0.163
			$\frac{1}{2}$	$\frac{1}{2}$	412.74	−0.31	0.50	−0.163
	$-\frac{1}{2}$	$\frac{1}{2}$	$\frac{1}{2}$	$\frac{1}{2}$	456.62	−0.90	1.00	−0.146
			$-\frac{1}{2}$	$-\frac{1}{2}$	460.32	−0.16	1.00	−0.146
$+ \leftarrow -$	$2\frac{1}{2}$	$1\frac{1}{2}$	$-\frac{1}{2}$	$-\frac{1}{2}$	944.05	−0.90	1.00	0.176
			$\frac{1}{2}$	$\frac{1}{2}$	946.98	−0.87	1.00	0.176
	$1\frac{1}{2}$	$\frac{1}{2}$	$-\frac{1}{2}$	$-\frac{1}{2}$	1030.1	−0.72	0.50	0.160
			$\frac{1}{2}$	$\frac{1}{2}$	1031.5	1.05	0.50	0.160
159.0 μm spectrum	$^2\Pi_{1/2}$,	$J = 4\frac{1}{2} \leftarrow 3\frac{1}{2}$	$\nu_L = 1885.9593$ GHz					
Parallel polarization (π)	No transitions observed below 2.0 T							
Perpendicular polarization (σ)								
$+ \leftarrow -$	$-\frac{1}{2}$	$\frac{1}{2}$	c		543.39	0.37	0.562	−0.153
	$-1\frac{1}{2}$	$-\frac{1}{2}$	c		562.55	−0.28	0.562	−0.148
	$-2\frac{1}{2}$	$-1\frac{1}{2}$	c		583.61	−0.11	0.562	−0.143
	$-3\frac{1}{2}$	$-2\frac{1}{2}$	c		606.92	−0.10	0.562	−0.137
	$-4\frac{1}{2}$	$-3\frac{1}{2}$	c		632.93	0.47	0.562	−0.131
$- \leftarrow +$	$-\frac{1}{2}$	$\frac{1}{2}$	c		1259.67	0.29	0.562	−0.154
	$-1\frac{1}{2}$	$-\frac{1}{2}$	c		1297.28	−0.16	0.562	−0.150
	$-2\frac{1}{2}$	$-1\frac{1}{2}$	c		1339.91	0.51	0.562	−0.145
	$-3\frac{1}{2}$	$-2\frac{1}{2}$	c		1388.62	0.02	0.562	−0.139
	$-4\frac{1}{2}$	$-3\frac{1}{2}$	c		1444.82	−0.21	0.562	−0.133
256 μm spectrum	$^2\Pi_{3/2}$,	$J = 2\frac{1}{2} \leftarrow 1\frac{1}{2}$	$\nu_L = 1170.9410$ GHz					
Parallel polarization (π)								
$- \leftarrow +$	$-1\frac{1}{2}$	$-1\frac{1}{2}$	c		142.20	−0.12	1.0	0.983
$+ \leftarrow -$	$-1\frac{1}{2}$	$-1\frac{1}{2}$	c		208.74	−0.48	1.0	0.984
$- \leftarrow +$	$-\frac{1}{2}$	$-\frac{1}{2}$	c		420.88	−0.48	1.0	0.337
$+ \leftarrow -$	$-\frac{1}{2}$	$-\frac{1}{2}$	c		613.78	−0.05	1.0	0.337
Perpendicular polarization (σ)								
$- \leftarrow +$	$-\frac{1}{2}$	$-1\frac{1}{2}$	$\frac{1}{2}$	$\frac{1}{2}$	106.45	−0.10	0.5	1.31
			$-\frac{1}{2}$	$-\frac{1}{2}$	106.79	−0.13	0.5	1.31
$+ \leftarrow -$	$-\frac{1}{2}$	$-1\frac{1}{2}$	$\frac{1}{2}$	$\frac{1}{2}$	156.17	0.13	0.5	1.31
			$-\frac{1}{2}$	$-\frac{1}{2}$	156.51	0.06	0.5	1.31
$- \leftarrow +$	$\frac{1}{2}$	$-\frac{1}{2}$	$\frac{1}{2}$	$\frac{1}{2}$	212.26	−0.86	0.5	0.660
			$-\frac{1}{2}$	$-\frac{1}{2}$	212.80	−0.72	0.0	0.660
	$-2\frac{1}{2}$	$-1\frac{1}{2}$	c		213.71	−0.83	1.0	0.655
$+ \leftarrow -$	$\frac{1}{2}$	$-\frac{1}{2}$	$\frac{1}{2}$	$\frac{1}{2}$	310.41	−0.14	0.5	0.664
			$-\frac{1}{2}$	$-\frac{1}{2}$	310.93	0.00	0.5	0.664
	$-2\frac{1}{2}$	$-1\frac{1}{2}$	c		314.41	−0.30	1.0	0.653
184.3 μm spectrum	$^2\Pi_{3/2}$,	$J = 3\frac{1}{2} \leftarrow 2\frac{1}{2}$	$\nu_L = 1626.6026$ GHz					
Parallel polarization (π)								
$+ \leftarrow -$	$2\frac{1}{2}$	$2\frac{1}{2}$	c		1253.80	0.96	0.750	−0.522
Perpendicular polarization (σ)								
$+ \leftarrow -$	$3\frac{1}{2}$	$2\frac{1}{2}$	c		1597.33	2.48	0.750	−0.411

TABLE II (*continued*).

Parity[a]	M_J'	M_J	M_I'	M_I	Flux density (mT)	$\nu_L - \nu_{calc}$[b] (MHz)	Weight (MHz^{-2})	$\partial\nu/\partial B_0$[b] (MHz/G)
183.6 μm spectrum	$^2\Pi_{3/2}$,	$J = 3\frac{1}{2} \leftarrow 2\frac{1}{2}$		ν_L = 1632.6669 GHz				
Parallel polarization (π)								
$+ \leftarrow -$	$2\frac{1}{2}$	$2\frac{1}{2}$	c		103.35	0.19	0.750	−0.532
$- \leftarrow +$	$-2\frac{1}{2}$	$-2\frac{1}{2}$	c		125.72	0.90	0.750	0.533
$+ \leftarrow -$	$1\frac{1}{2}$	$1\frac{1}{2}$	c		172.14	−0.29	0.750	−0.319
$- \leftarrow +$	$-1\frac{1}{2}$	$-1\frac{1}{2}$	c		209.76	−0.07	0.750	0.320
$+ \leftarrow -$	$\frac{1}{2}$	$\frac{1}{2}$	c		517.9	−0.54	0.750	−0.106
$- \leftarrow +$	$-\frac{1}{2}$	$-\frac{1}{2}$	c		625.8	0.66	0.750	0.108
Perpendicular polarization (σ)								
$- \leftarrow +$	$-1\frac{1}{2}$	$-2\frac{1}{2}$	c		103.5	−1.92	0.750	0.650
$+ \leftarrow -$	$\frac{1}{2}$	$1\frac{1}{2}$	c		126.6	0.09	0.750	−0.434
$+ \leftarrow -$	$3\frac{1}{2}$	$2\frac{1}{2}$	c		131.73	−0.24	0.750	−0.417
$- \leftarrow +$	$-\frac{1}{2}$	$-1\frac{1}{2}$	c		153.5	0.18	0.750	0.437
$- \leftarrow +$	$-3\frac{1}{2}$	$-2\frac{1}{2}$	c		161.34	0.28	0.750	0.415
$+ \leftarrow -$	$2\frac{1}{2}$	$1\frac{1}{2}$	c		269.2	0.09	0.750	−0.204
$- \leftarrow +$	$\frac{1}{2}$	$-\frac{1}{2}$	c		299.7	−0.03	0.750	0.224
$- \leftarrow +$	$-2\frac{1}{2}$	$-1\frac{1}{2}$	c		331.2	−0.07	0.750	0.202
117.7 μm spectrum	$^2\Pi_{3/2}$,	$J = 5\frac{1}{2} \leftarrow 4\frac{1}{2}$		ν_L = 2546.4950 GHz				
Parallel polarization (π)								
$- \leftarrow +$	$4\frac{1}{2}$	$4\frac{1}{2}$	c		127.0	−0.44	0.308	−0.203
	$3\frac{1}{2}$	$3\frac{1}{2}$	c		164.1	0.59	0.308	−0.158
	$2\frac{1}{2}$	$2\frac{1}{2}$	c		229.5	0.03	0.308	−0.111
	$1\frac{1}{2}$	$1\frac{1}{2}$	c		383.2	−0.20	0.308	−0.067
	$\frac{1}{2}$	$\frac{1}{2}$	c		1187.0	0.12	0.0	−0.021
$+ \leftarrow -$	$4\frac{1}{2}$	$4\frac{1}{2}$	c		1385.0	−1.94	0.308	−0.201
	$3\frac{1}{2}$	$3\frac{1}{2}$	c		1786.5	−0.30	0.308	−0.155
Perpendicular polarization (σ)								
$- \leftarrow +$	$5\frac{1}{2}$	$4\frac{1}{2}$	c		115.58	0.09	0.308	−0.224
$+ \leftarrow -$	$5\frac{1}{2}$	$4\frac{1}{2}$	c		1237.26	−0.68	0.308	−0.227
	$4\frac{1}{2}$	$3\frac{1}{2}$	c		1548.0	1.72	0.308	−0.182

[a] The parity of the upper state is given first.
[b] Calculated value obtained using the parameter values in Table III.
[c] Proton hyperfine structure not resolved.

tion frequency[3] with the laser frequency. Given reasonable estimates of smaller molecular parameters, it was possible to match the predictions of the computer program (which calculates all possible Zeeman transitions above a selected intensity) with the experimental spectra and thus to make the assignments directly. The full details of the experimental measurements and their assignments are given in Table II.

Some insight into the observed Zeeman patterns can be obtained from a consideration of the g_J factors for the rotational levels involved. To a good approximation, the Zeeman effect is linear and described by

$$E_Z = g_J \mu_B B_0 M_J, \tag{1}$$

where μ_B is the Bohr magneton, B_0 the applied flux density, and M_J the quantum number associated with the component of the total angular momentum J along the magnetic field direction. A second order perturbation treatment of the major terms involved for a molecule in a $^2\Pi$ state gives

$$F_1(^2\Pi_{1/2}) \text{ component} \quad g_J = \frac{2B\left[(J+\frac{1}{2})^2 - 1\right]}{(A-2B)J(J+1)}, \tag{2a}$$

$F_2(^2\Pi_{3/2})$ component

$$g_J = \frac{3}{J(J+1)} - \frac{2B\left[(J+\frac{1}{2})^2 - 1\right]}{(A-2B)J(J+1)}, \tag{2b}$$

where A is the spin-orbit coupling parameter and B the rotational constant. The values for the g_J factors for SiH in its first few rotational levels, calculated from these formulas, are given in Table III. Two features of the values obtained are of especial interest. First, for the molecule in its $^2\Pi_{1/2}$ component, the g_J factor arises from the rotational admixture of the $^2\Pi_{3/2}$ component (with the exception of the unique level $J = 1/2$). The value obtained is essentially J independent, as may be seen from the table. It is therefore readily appreciated why no spectrum for $^2\Pi_{1/2}$ transitions in SiH was recorded in π polarization (i.e., with $\Delta M_J = 0$),

TABLE III. Calculated g_J factors for SiH in low-lying levels of its $X\,^2\Pi$ state.

J	g_J − value[a] $^2\Pi_{1/2}$	$^2\Pi_{3/2}$
$\frac{1}{2}$	0.0	...
$1\frac{1}{2}$	0.0923	0.7077
$2\frac{1}{2}$	0.1055	0.2374
$3\frac{1}{2}$	0.1099	0.0806
$4\frac{1}{2}$	0.1119	0.0093
$5\frac{1}{2}$	0.1130	−0.0291

[a] Values calculated from the formulas given in Eqs. (2a) and (2b), with $A = 142.855\ cm^{-1}$, $B = 7.389\,72\ cm^{-1}$, i.e., $2B/(A-2B) = 0.1154$.

apart from the 479.9 μm spectrum which involves the $J = 1/2$ level. Secondly, although the g_J factors for the $^2\Pi_{3/2}$ levels decrease sharply with J in accordance with expectation for a molecule in a Hund's case (a) $^2\Pi$ state, the spin uncoupling term causes the g_J factor to change sign between $J = 4\frac{1}{2}$ and $5\frac{1}{2}$. For the $J = 5\frac{1}{2} \leftarrow 4\frac{1}{2}$ transition therefore (detected with the 117.7 μm laser line), the g_J factor for the upper level is larger in magnitude than that for the lower level, a rather unusual situation. It is this characteristic which causes the strongest M_J transitions to occur at lowest field in the 117.7 μm σ spectrum, for example.

Reference to Fig. 1 shows that no fine structure transitions between the two spin components, $^2\Pi_{3/2}$ and $^2\Pi_{1/2}$ were observed. Apart from the fact that these transitions are intrinsically weaker, we were unable to discover any convenient near coincidences with available laser lines for them. This is particularly unfortunate since, without such an observation, the spin orbit coupling constant A cannot be determined directly. It may be seen from the diagram in Fig. 1 that the $J = 3\frac{1}{2}$, $^2\Pi_{3/2}$ level and the $J = 5\frac{1}{2}$, $^2\Pi_{1/2}$ level are very close in energy. Detailed calculations reveal that the + parity component of the $J = 3\frac{1}{2}$ level lies some 5 GHz above that of the $J = 5\frac{1}{2}$ level. The possibility exists, therefore, that anticrossings betwen the M components of these states can be observed in our experiments, which would provide an alternative determination of A. Such anticrossings would be weak because the two rotational levels involved are not connected directly by the Zeeman interaction. Reference to Table III shows that the g_J factors for the two levels concerned are very similar, with the value for the $^2\Pi_{1/2}$ components slightly the larger (somewhat unexpectedly). This is unfortunate because it means that even for the most rapidly tuning levels ($M_J = 3\frac{1}{2}$) the anticrossing occurs at rather higher fields (3.15 T), beyond the range of the magnet of the LMR apparatus. Our main observations of the $J = 3\frac{1}{2} \leftarrow 2\frac{1}{2}$, $^2\Pi_{3/2}$ transition were made with the laser line at 183.6 μm but we also measured a few resonances for the same rotational transition with the 184.3 μm laser (ssee Table II). The latter laser frequency allows observations of transitions at higher fields, much closer to the predicted anticrossings. It was hoped that such measurements would reveal the mixing of the two rotational levels by the magnetic field. Although this hope was realised, subsequent numerical calculations showed that the effects were too small to improve our knowledge of the spin-orbit coupling constant significantly.

IV. LEAST-SQUARES FIT

The data listed in Table II have been fitted to a $^2\Pi$ Hamiltonian, cast in the N^2 formulation as defined in Ref. 15. The parameter A_D was set to zero in order to avoid the problems of indeterminancies. Consequently, the parameters determined in the fit, notably A, γ, and B, must be regarded as effective parameters; this is indicated by tildes in Table IV. The data set in Table II is not sufficient to determine all the parameters in the Hamiltonian and some have been constrained to values determined by other means. We have chosen to constrain the spin-orbit parameter A to the value determined from the $A\,^2\Delta$–$X\,^2\Pi$ optical spectrum.[3] Although the precision of measurement of the optical lines (0.005 cm^{-1}), is much inferior to that for the far infrared (1 MHz or 3×10^{-5} cm^{-1}), the electronic spectrum allows a direct measurement of the spin-orbit splitting whereas the present data are affected only indirectly. Thus the values for the parameters determined in our fit are relatively insensitive to the value adopted for A.

TABLE IV. Parameters for ^{28}SiH in the $v = 0$ level of the $X\,^2\Pi$ state.[a]

$\tilde{A} + \tilde{\gamma}$	4 282 350.2[b]	B	221 598.534(32)
$\tilde{\gamma}$	− 1 390.08(50)[c]	D	12.026 51(97)
γ_D	0.352(22)	10^3H	0.444 1[b]
$p + 2q$	2 999.75(48)	q	251.268(65)
$p_D + 2q_D$	− 0.567(15)	$10q_D$	− 0.531[b]
$h_{1/2}$	34.3(15)	b	− 48.3[b]
$h_{3/2}$	4.68[b]	d	17.9(13)
g'_L	1.000 11(12)	10^2g_r	− 0.147 3(17)
g_S	2.002 0[b]	$10^2(g'_l - g^{e'}_r)$	0.676 8[b]
10^2g_l	0.315 7[b]	$10^2g^{e'}_r$	− 0.113 4[b]

[a] Value in MHz, where appropriate.
[b] Parameter constrained to this value in the least squares fit.
[c] The numbers in parenthesis represent one standard deviation of the least-squares fit, in units of the last quoted decimal place.

The value for the sextic centrifugal distortion constant H was estimated from the formula

$$H_0 \sim H_e = \tfrac{2}{3}D_e\{12(B_e/\omega_e)^2 - \alpha_e/\omega_e\}, \tag{3}$$

where the subscript e denotes the equilibrium value and ω_e and α_e are the harmonic vibrational frequency and the anharmonic correction to the rotational constant, respectively. The centrifugal distortion correction to the lambda doubling parameter q was estimated from

$$q_D = -4qD/B \tag{4}$$

which has been found to hold well for CH.[16]

Six independent g factors are required to describe the Zeeman effect for a molecule in a $^2\Pi$ state,[17] discounting the nuclear spin term. We find in practice that only two of these are determinable for SiH. Values for the other four are estimated from the following relations:

$$g_S = 2.0023 - \delta g_{\rm rel}, \tag{5}$$

$$g_l = -\gamma/2B, \tag{6}$$

$$g'_l = p/2B, \tag{7}$$

$$g^{e'}_r = -q/B. \tag{8}$$

Previous work[8] suggests that, of these, only Curl's relationship [Eq. (6)] is likely to be at all unreliable. Fortunately, this parameter does not have a very strong effect on the observations in the LMR spectrum.

As has been mentioned earlier, the proton hyperfine splitting was only resolved in some of the spectra recorded in this work. Consequently, it has not been possible to determine values for all the four parameters required to describe the magnetic hyperfine interaction.[18] At the start of our analysis, we estimated values for these parameters by scaling the corresponding values for SH.[19] The parameters a, c, and d were scaled as the inverse cube of the bond length while the Fermi contact parameter b_F was reduced in the same ratio as

the corresponding parameters for CH and OH. The latter is obviously a rather doubtful assumption but, in the absence of any *ab initio* calculations, it is hard to come up with a better estimate. The values obtained were

$$a = 22.4 \text{ MHz}, \quad b = -48.3 \text{ MHz},$$
$$c = 22.3 \text{ MHz}, \quad d = 18.8 \text{ MHz}.$$

The hyperfine splittings for levels in the $^2\Pi_{1/2}$ and $^2\Pi_{3/2}$ components are determined by combinations of these parameters,

$$h_{1/2} \equiv a - \tfrac{1}{2}(b + c) = 35.4 \text{ MHz}, \tag{9}$$
$$h_{3/2} \equiv a + \tfrac{1}{2}(b + c) = 9.4 \text{ MHz}, \tag{10}$$

respectively. As a consequence of these different magnitudes, the hyperfine splittings were fully resolved for all transitions involving the $^2\Pi_{1/2}$ levels but only in a few favorable cases for $^2\Pi_{3/2}$ transitions. The value for $h_{3/2}$ was therefore adjusted to reproduce these splittings in the $^2\Pi_{3/2}$ transitions and constrained to this value in the least-squares fit.

The basis set in the calculation was truncated without loss in accuracy at $\Delta J = \pm 1$. Each datum was weighted inversely as the square of the estimated experimental error in the fit; the weights are given in Table II. The main contribution to the error comes from the uncertainty in knowledge of the far-infrared laser frequencies ($\sim 5 \times 10^{-7}$). The results of the fits are given in Table II and the parameter values determined in the process are given in Table IV. The standard deviation of the fit relative to the experimental uncertainty was 0.638, a value which is slightly too good and suggests that the weights may have been chosen a little pessimistically. In fact, recent remeasurements of the laser frequencies show that the uncertainties in their values are about half those given in Table I.

V. DISCUSSION

The present observations and the parameters given in Table IV represent a considerable improvement in our knowledge of the energy levels of SiH in its ground $^2\Pi$ state. Nevertheless, for the most part the parameter values are consistent with those determined in previous work[3]:

$$\tilde{B} = 221\,589(2) \text{ MHz}, \quad D = 11.98(12) \text{ MHz},$$
$$p = 2486(10) \text{ MHz}, \quad q = 248.4(14) \text{ MHz}.$$
$$\tilde{\gamma} = 1397(18) \text{ MHz},$$

(These values were obtained in a refit of the optical data to the effective Hamiltonian used in the present study and so differ slightly from those given in the original paper).[3] The numbers which are perhaps of most immediate interest are the lambda-type doubling intervals since these define the frequencies at which radio astronomers should search for SiH in the interstellar gas clouds. A complete set of these frequencies have been published elsewhere[11] but for the lowest rotational level $J = 1/2$ the values are

$$F = 0^- - 1^+ \quad \nu = 2969.7 \text{ MHz},$$
$$1^- - 1^+ \quad \nu = 3004.6 \text{ MHz},$$
$$1^- - 0^+ \quad \nu = 3015.6 \text{ MHz}.$$

Both components of the lambda doublet are involved in the lines recorded with the 479.9 μm laser so that a fairly direct measurement of their separation has been possible. We estimate the uncertainty in the lambda doubling frequencies to be about 2 MHz. The value for the lambda doubling parameter $(p + 2q)$ agrees almost exactly with the value obtained earlier by Cooper and Richards,[20] a remarkable tribute to their calculations. However, the *ab initio* value for q(270.3 MHz) does not agree quite so well. Our value for $(p + 2q)$ is about 30 MHz larger than that obtained from the optical spectrum.[3]

The parameter γ_D was required in the fit to remove certain systematic residuals. The value obtained does not agree very well with the estimate of 0.151 MHz obtained from the relationship

$$\gamma_D = -2\gamma D / B. \tag{11}$$

However, this formula is not thought to be very reliable. Furthermore our value is consistent with that determined by the optical data of 0.47(12) MHz.

The values for the proton hyperfine parameters given in Table IV agree quite well with the estimates given earlier in Eqs. (9), (10), and above, which suggests that the scaling procedures employed are reasonably reliable for SiH. It should be appreciated that the parameter set is not completely determined by the data. The values obtained depend fairly strongly on the value assumed for b because spin-uncoupling effects are quite pronounced for this molecule.

Mention has been made earlier of the surprising weakness of the LMR spectrum of SiH and our inability to saturate the transitions. Soon after the observation of the spectra reported here, silicon atoms were detected with good signal-to-noise in the same F + SiH_4 flame, also by LMR spectroscopy at far-infrared wavelengths.[21] This observation corresponds to the detection of similar abundances of C atoms in the F + CH_4 flame[22] and suggests that the chemical reactions are much the same in the two cases. This is additional evidence that the weakness of the spectrum cannot be attributed to low SiH concentrations. On the other hand, it is explicable by a small value for the electric dipole moment of SiH in the $v = 0$ level of the $X\,^2\Pi$ state, a suggestion which is supported by a recent *ab initio* estimate of 0.124 D.[23] We have been able to measure the magnitude of the dipole moment for GeH from the relative intensities of electric and magnetic dipole transitions in its LMR spectrum[10]; the value obtained is 1.24 D. There is thus a rather intriguing variation in the dipole moment down the series CH, SiH, and GeH (1.46,[24] 0.124, and 1.24 D).

[1] A. E. Douglas and G. A. Elliot, Can J. Phys. **43**, 496 (1965).
[2] L. Klynning and B. Lindgren, Ark. Fys. **83**, 73 (1967).
[3] L. Klynning, B. Lindgren, and U. Sassenberg, Phys. Scr. **20**, 617 (1979).
[4] K. M. Evenson, Discuss. Faraday Soc. **71**, 7 (1981).
[5] P. B. Davies, J. Phys. Chem. **85**, 2559 (1981).
[6] K. M. Evenson, H. E. Radford, and M. M. Moran, Jr., Appl. Phys. Lett. **18**, 426 (1971).
[7] J. T. Hougen, J. A. Mucha, D. A. Jennings, and K. M. Evenson, J. Mol. Spectrosc. **72**, 463 (1978).
[8] J. M. Brown and K. M. Evenson, J. Mol. Spectrosc. **98**, 392 (1983).
[9] T. J. Sears, P. R. Bunker, A. R. W. McKellar, K. M. Evenson, D. A. Jennings, and J. M. Brown, J. Chem. Phys. **77**, 5348 (1982).
[10] J. M. Brown, K. M. Evenson, and T. J. Sears (to be published).

[11]J. M. Brown, R. F. Curl, and K. M. Evenson, Astrophys. J. Lett. (in press).
[12]J. M. Brown and D. Robinson, Mol. Phys. **51**, 883 (1984).
[13]J. C. Knights, J. P. M. Schmitt, J. Perrin, and G. Guelachvili, J. Chem. Phys. **76**, 3414 (1982).
[14]J. M. Brown, C. M. L. Kerr, F. D. Wayne, K. M. Evenson, and H. E. Radford, J. Mol. Spectrosc. **86**, 544 (1981).
[15]J. M. Brown, E. A. Colbourn, J. K. G. Watson, and F. D. Wayne, J. Mol. Spectrosc. **74**, 294 (1979).
[16]C. R. Brazier and J. M. Brown, Can. J. Phys. (in press).
[17]J. M. Brown, M. Kaise, C. M. L. Kerr, and D. J. Milton, Mol. Phys. **36**, 553 (1978).
[18]R. A. Frosch and H. M. Foley, Phys. Rev. **88**, 1337 (1952).
[19]W. L. Meerts and A. Dymanus, Can. J. Phys. **53**, 2123 (1975).
[20]D. L. Cooper and W. G. Richards, J. Chem. Phys. **74**, 96 (1981).
[21]M. Inguscio, K. M. Evenson, V. Beltran-Lopez, and E. Ley-Koo, Astrophys. J. Lett. **278**, L127 (1984).
[22]R. J. Saykally and K. M. Evenson, Astrophys. J. **238**, L107 (1980).
[23]M. Lewerenz, P. J. Bruna, S. D. Peyerimhoff, and R. J. Buenker, Mol. Phys. **49**, 1 (1983).
[24]D. H. Phelps and F. W. Dalby, Phys. Rev. Lett. **16**, 3 (1966).